Chaos, Solitons and Fractals 152 (2021) 111306

Contents lists available at ScienceDirect

Chaos, Solitons and Fractals

Nonlinear Science, and Nonequilibrium and Complex Phenomena

journal homepage: www.elsevier.com/locate/chaos

A simple fractional-order chaotic system based on memristor and memcapacitor and its synchronization application

Akif Akgül[a], Karthikeyan Rajagopal[b], Ali Durdu[c], Muhammed Ali Pala[d,*], Ömer Faruk Boyraz[e], Mustafa Zahid Yildiz[d]

[a] Department of Computer Engineering, Faculty of Engineering, Hitit University, Corum, 19030, Turkey
[b] Center for Nonlinear Systems, Chennai Institute of Technology, Chennai, India
[c] Faculty of Political Sciences, Department of Business Administration, Management Information Systems, Social Sciences University of Ankara, Ankara, 06050, Turkey
[d] Department of Electrical and Electronics Engineering, Faculty of Technology, Sakarya University of Applied Sciences, Sakarya, 54050, Turkey
[e] Anadolu Isuzu Automotive Industry and Trade Inc., Research and Development Center, Kocaeli, Turkey

ARTICLE INFO

Article history:
Received 2 April 2021
Revised 17 July 2021
Accepted 28 July 2021

Keywords:
Chaos
Fractional-order chaotic systems
Memcapacitor and memristor
Dynamical analysis
Synchronization application

ABSTRACT

Memelements play an important part in the design of high density memory systems and low power memory. In this paper, we created a novel fractional-order chaotic circuit with a memristor and a memcapacitor with a linear inductor. The various dynamical properties of the fractional-order system are investigated by using some dynamic analysis methods like Lyapunov exponents and bifurcation after the numerical solution for the fractional-order system. In addition, to show the applicative advantages of the proposed chaotic system, we have realized about the synchronization of fractional-order chaotic systems and used it in secure communication systems first time in the literature according to our knowledge. The results of the theoretical analysis and simulation show that the simple fractional-order chaotic system has very rich dynamic properties and can be used in different engineering applications.

1. Introduction

Memristor was proposed as a two-terminal circuit element by Leon Chua in 1971 [1] that relates electrical charge to magnetic flux and was first physically manufactured at the HP Laboratory in 2008 [2].The memristor has been used in many memristor-based design applications in the literature with its characteristic features, such as computer architectures, neuromorphic structures, and digital circuits [3–7]. One of these application areas is memristor-based chaotic systems. Its nonlinear feature has shown that the memristor can be used in chaotic circuits, and recently the design of memristor-based chaotic circuits with various nonlinear equations has received considerable attention. Several memristor-based chaotic/hyper-chaotic circuits have been developed and extensively explored in recent years, using memristors instead of nonlinear resistors used in classical chaotic circuits [8–11].The numerical simulation of such intricate systems are discussed in few literatures [12,13] and identified with challenges in obtaining results. In [6,14–18] stochastic models with memelements and significance of hysteresis effect in dynamic behavior were discussed.

Zhou et al. suggested a smooth nonlinear four-wing hyper-chaotic system by introducing only a flux-controlled memristor to a pseudo-four-wing, three-dimensional (3D) chaotic structure. The dynamic behavior of the new memristive system, in which the circuit is also developed, has been confirmed by theoretical analysis and simulation. With the proposed system, four-wing attractors were produced, and thanks to this system, it can also produce from two to four-wing chaotic attractors by adjusting the parameter [19,20]. Ma et al. suggested the application of a flux-controlled memristor to a three-dimensional autonomous chaotic system as a new hyper-chaotic attractor. The transition from chaos to hyper-chaos has been observed as the control parameters in the system decreased. Additionally, it was shown thatit was shown that the hyper-chaotic state persists throughout the entire process. As a consequence of the experiments, it was shown that the newly developed method has a richer dynamic nature than other literature studies [21].

Bao et al. engineered an unbalanced hyper-chaotic memristive system that combines an infinite number of hidden attractors, using a memristor instead of a coupling resistor in a three-

* Corresponding author.
E-mail address: pala@subu.edu.tr (M.A. Pala).

https://doi.org/10.1016/j.chaos.2021.111306
0960-0779/

dimensional chaotic system's realization circuit. Hardware tests and simulations of Power Simulation (PSIM) circuits were performed to check the simulation results of the system developed [22]. Li et al. modified the 3-dimensional chaotic system developed by Lu and Chen [23] and transformed it into a 4-dimensional memristive chaotic system. While the system maintained its symmetry after the modification process, it was added to the new system in abundantly complex dynamics, such as boundary loops, chaos, and even hyperchaos. The developed system has an infinite number of stable equilibria that cannot be counted in comparison with other studies in the literature [24]. Njitacke et al. have developed a new system by replacing the memristive diode bridge on the circuit they made before [25] with a flux-controlled memristor. The new memristor oscillator developed has been described as a continuous-time autonomous system with a four-dimensional balance line. The analyzes of the realized system were carried out using the bifurcation diagram, Poincar sections, and graphics of Lyapunov bases. It was simulated on PSIM to verify that an infinite number of attractors were formed from the developed system [26].

Kuate et al. proposed a new non-equilibrium hyper-chaotic system using the Lorenz equations. A low-cost microcontroller was used to make the developed system in real-time. The system is explained with a very simple mathematical model. The difference from other Lorenz-based systems is that there are no balance points. The system also differs from other memristive chaotic systems in that it has very long-lasting transient chaotic states, versatility, and three different erupting oscillation modes [27]. Sahin et al. have developed a 4-dimensional chaotic system with flux-controlled memristor. It has been observed that two optimization methods solve the synchronization problems of chaotic circuits. As a result, an optimized Proportional-Integral-Derivative controlled chaotic circuit and the information signal masked on the transmitter are recovered with the chaotic system in the receiver, and a secure communication system is designed [28].

Most of the literatures discussed chaotic circuits with memristor, memcapacitor or meminductor but only few were reported circuits with combination of these mem-elements. The complications in circuit implementation and challenges in dynamical analysis methods made the progress slowdown in this research direction [29,30]. In [31] a simple chaotic circuit with meminductor a linear resistor and a linear capacitor is presented and brings out rich dynamical behaviors as well as showed the circuit hardware realizable. A chaotic circuit designed with two memcapacitors is investigated and portrayed with three different attractors, circuit implementation also carried out [32]. This discussion lay a platform to us towards proposing a simple chaotic circuit with combination of mem-elements. Configuration of systems with noise effects and influence of electromagnetic flux were investigated in [33–37] the results laid a platform to refine the dynamic analysis with experimental values.

The basic property of memristor is its pinched hysteresis loop or remembrance of previous states hence the chaotic circuits with memristor needs to be analyzed with a tool which consider memory effects and provide more degree of freedom for analysis. Fractional calculus is identified with advantages of such kinds and it can be considered as generalization of method to describe the characteristics including integer-order values. The differential equations formulated with fractional derivatives enhanced the degree of freedom of the system with more fractional parameters. Recent studies reveled many unidentified characteristics such as variable-boostable feature, chaos bursting phenomenon, phase diagram offsets, coexisting attractors, and transient and local sustained chaotic states are exposed while the model treated with fractional calculus.

Rajagopal et al. in their study, explored the dynamic properties of memcapacitor-based chaotic oscillator's and obtained and analyzed its fractional-order model. They improved the hyper-chaotic memcapacitor oscillator fractional-order model. The developed oscillator was integrated into Field Programmable Gate Arrays [38]. Li et al. have developed an algorithm on encrypting RGB images by using DNA sequence operations with a fractional-order 4-D hyper-chaotic memristive system. The images encrypted as a result of the algorithm have been successfully passed through security analysis [39].

In a different study, Tsafack et al. crafted a new 4-dimensional chaotic circuit by replacement an RLCC-diode-opamp with an analogous hybrid memristive circuit. The difference in the literature from the recent studies is that there are six and four disconnected chaotic attractors. A chaos-based image encryption algorithm has been developed using S-Box and Pseudo Random Number Generator from the chaotic series of attractors. With the developed chaotic encryption algorithm, it has been proved with various analyzes that the gray level and color images are successfully encrypted [40]. Toopchi and Wang proposed a synchronization application of hyper-chaotic Zhou systems [41]. Lu et al. proposed the synchronization of a unified chaotic system and the application in secure communication [42]. Memristor-based fractional-order competitive neural networks is studied with and without the inclusion of impulsive effects and the results revealed fractional-order treatment can expose different dynamical properties of the system while integer-order treatment is no longer useful to analyze memristor based chaotic circuits [43].

In this study, we focus on a fractional-order chaotic circuit with a memristor and a memcapacitor with a linear inductor. The various dynamical properties of the fractionalorder system are investigated by using some dynamic analysis methods such as Lyapunov exponents and bifurcation after the numerical solution for the fractional-order system. Numerical solution for the fractional-order system and the fractional memristor-fractional memcapacitor circuit (FMFMC) model in section 2, dynamical properties of the FMFMC system in section 3, synchronization of FMFMC system in section 4 and finally the conclusion are presented.

2. The Fractional Memristor-Fractional Memcapacitor Circuit (FMFMC) model

By using the current through inductor, the internal state of memristor, the electromagnetic flux and the internal state variable of the memcapacitor the state equations of the memristor-memcapacitor circuit was derived in appendix-1 using some definitions from [44] as,

$$\begin{aligned} \dot{i}_L &= \frac{1}{L} M_C^q \phi \\ D^q y &= -a_2 M_C^q \phi - a_3 y + a_4 M_C^{q^2} \phi^2 y \\ D^q \phi &= -i_L - M_R^q M_C^q \phi \\ D^q w &= \phi \\ M_C^q &= \alpha + \beta w \\ M_R^q &= \chi y^2 - \delta \end{aligned} \tag{1}$$

where i_L, y, ϕ, w denotes the current through the inductor, memristor internal state, the flux and state variable of the memcapacitor respectively while M_C^q, M_R^q are the memcapacitor and memristor functions [44]. In the [44], it was considered that both memristor and memcapacitor are integer-order elements as shown in Fig 1. It was in [45] that the authors have discussed about the importance of fractional-order analysis in devices such as memristor. Hence by using fractional-order memristor and memcapacitor [46,47] we have derived the state equations as in (1).

To derive the dimensionless model we redefine the state variables as $i_L = x;\ \phi = z$ the Fractional Memristor-Fractional Memca-

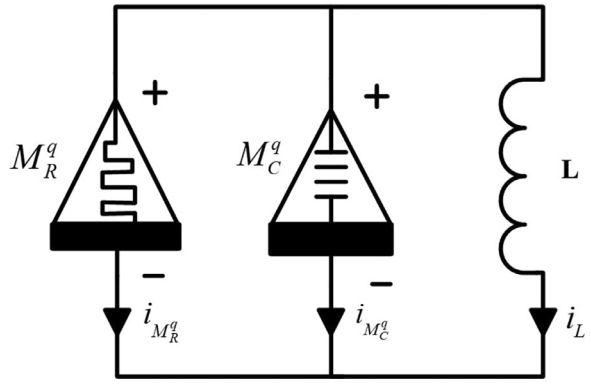

Fig. 1. The simple chaotic circuit with fractional-order memristor (M_R^q) and memcapacitor (M_C^q).

pacitor circuit (FMFMC) can be modified from (1) as,

$$\begin{aligned}
&\dot{x} = a_1 M_C^q z = F_x \\
&D^q y = -a_2 M_C^q z - a_3 y + a_4 M_C^{q^2} z^2 y = F_y \\
&D^q z = -x - M_R^q M_C^q z = F_z \\
&D^q w = z = F_w \\
&M_C^q = \alpha + \beta w \\
&M_R^q = \chi y^2 - \delta
\end{aligned} \tag{2}$$

The other parameters values used in the simulations are given in (3)

$$\begin{aligned}
&a_1 = 0.01; a_2 = 0.5; a_3 = 0.54; a_4 = 4; \\
&\alpha = \beta = 1; \chi = 0.001; \delta = 0.005;
\end{aligned} \tag{3}$$

There has been several methods to numerically solve the incommensurate fractional-order systems, but we have used the predictor-corrector method [48,49] to discretize the FMFMC system (2) and the predict-evaluate-correct-evaluate (PECE) method of Adams-Bashforth-Moulton studied in [50,51] is used. Let us define a generalized fractional-order differential equation as;

$$D^q y = f(t, y), 0 \le t \le T, \tag{4}$$

where $y^m(0) = y_0^m$ for $m \in (0, n-1)$ the initial point of (4) can be defined as;

$$y(t) = \sum_{m=0}^{n-1} y_0^m \frac{t^m}{m!} + \frac{1}{\Gamma(q)} \int_0^t \frac{f(\tau, y)}{(t-\tau)^{1-q}} d\tau. \tag{5}$$

For the numerical integration, we use the predictor-corrector method [48,49] whose predictor form at t_{m+1} is given by

$$y^P(t_{m+1}) = y_0 + \frac{1}{\Gamma(q)} \sum_{k=0}^{m} \beta_{k,m+1} f(y_{t_k}), \quad 0 \le t \le T, \tag{6}$$

and the corrector form can be defined by

$$y^C(t_{m+1}) = y_0 + \frac{h^q}{\Gamma(q+2)} \left\{ f\left(y^P_{t_{m+1}}\right) + \sum_{k=0}^{m} \alpha_{k,m+1} f(y_{t_k}) \right\} \tag{7}$$

where α and β are the corrector and predictor weight whose numerical values are calculated as;

$$\alpha_{k,m+1} = \frac{h^q}{q(q+1)} \begin{cases} m^{q+1} - (m-q)(m+1)^q, \\ k = 0 \\ (m-k+2)^{q+1} + (m-k)^{q+1} - 2(k-j+1)^{q+1}, \\ 1 \le k \le m \\ 1 \\ k = m+1 \end{cases}$$

$$\beta_{k,m+1} = \frac{h^q}{q} \left((m-k+1)^q - (m-k)^q \right). \tag{8}$$

The estimated error is $e = Max|z(t_k) - z_h(t_k)| = 0(h^p)$ while $k = 0, 1, \ldots, N$ and $p = Min(2, 1+q)$. The term $z_h(t_k)$ denotes the discrete form of (5) derived as defined in [46] as

$$\begin{aligned}
z_h(t_{n+1}) = &\sum_{k=0}^{n-1} z_0^{(k)} \frac{t_n^{k+1}}{k!} + \frac{h^q}{\Gamma(q+2)} f\left(t_{n+1}, z_h^p(t_{n+1})\right) \\
&+ \frac{h^q}{\Gamma(q+2)} \sum a_{j,n+1} f\left(t_j, z_h(t_j)\right)
\end{aligned} \tag{9}$$

The first state of the FMFMC system (2) is solved using the fourth-order Runge-Kutta (RK4) method and the other three fractional-order states are solved using PECE derived in (6-9). The discretized FMFMC system (2) can be derived as,

$$\begin{aligned}
&x(n+1) = x(n) + \frac{1}{6}\left[C_x^{(1)}(n) + 2C_x^{(2)}(n) + 2C_x^{(3)}(n) + C_x^{(4)}(n)\right] \\
&y(n+1) = \left\{ y(n) + \frac{h^q}{\Gamma(q+2)} F^P_{y_{n+1}} + \frac{h^q}{\Gamma(q+2)} \sum_{k=0}^{n} \left[\alpha_{k,n+1} F_{y_k}\right] \right\} \\
&z(n+1) = \left\{ z(n) + \frac{h^q}{\Gamma(q+2)} F^P_{z_{n+1}} + \frac{h^q}{\Gamma(q+2)} \sum_{k=0}^{n} \left[\alpha_{k,n+1} F_{z_k}\right] \right\} \\
&w(n+1) = \left\{ w(n) + \frac{h^q}{\Gamma(q+2)} F^P_{w_{n+1}} + \frac{h^q}{\Gamma(q+2)} \sum_{k=0}^{n} \left[\alpha_{k,n+1} F_{w_k}\right] \right\}
\end{aligned} \tag{10}$$

where q considering only the commensurate order case. The predictor and the corrector weight (α and β) are calculated using (6-9).The coefficients of the RK4 method ($C_x^{(i)}(n)$) are calculated and updated alongside the fractional-order responses for each iteration. In the entire paper, the step size used is h=0.01 and we have used the modified fde12 function [52] to have the algorithm work alongside RK4 to have the desired simulation results for the system defined in (9). In Fig. 2, we have shown the attractors for two different fractional-orders. In [44], the authors used combinations of parameters to achieve different attractors but including fractional-order will increase the topologically different attractors. In this case for a particular value of parameters as in [50], the integer-order system shows a single attractor with two scrolls whereas the fractional-order systems will show both single and two scroll attractors for the same parameter sets but with different initial conditions.

3. Dynamical properties of the FMFMC system

As mentioned in the previous section, we have used commensurate order for our analysis and various dynamical properties of the FMFMC system are investigated in the following subsections.

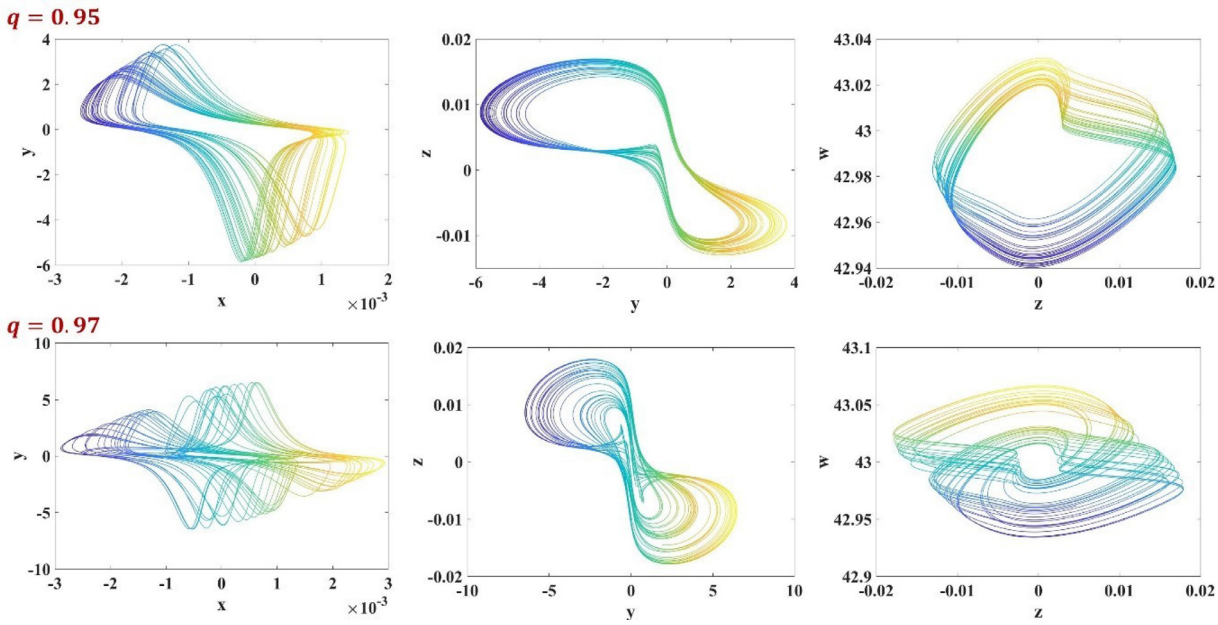

Fig. 2. 2D phase portraits of the FMFMC system for the initial conditions [0.1;0.1;0.1]. The phase plots are for two values of fractional-order q=0.95 and q=0.97. We could see that the FMFMC systems shows different attractors for the fractional-orders mentioned.

3.1. Stability of equilibrium points

It could be easily verified from that the FMFMC system has a line of equilibria given by $E_L = [0, 0, 0, w_e]$ derived equating the left hand side of (1) to zero. The generalized characteristic polynomial of the FMFMC system is calculated using the relation $\left|\left(diag(\lambda, \lambda^q, \lambda^q, \lambda^q) - J_{E_L}\right)\right| = 0$ which is derived using $q = 0.9$ as,

$$\begin{aligned}\lambda^{37} + a_3\lambda^{28} - \alpha\delta\lambda^{28} - \beta\delta\lambda^{28}w_e - a_3\alpha\delta\lambda^{19} - a_3\beta\delta\lambda^{19}w_e \\ + a_1\alpha\lambda^{18} + a_1\beta\lambda^{18}w_e + a_1a_3\alpha\lambda^{9} + a_1a_3\beta\lambda^{9}w_e\end{aligned} \tag{11}$$

The equilibrium point of the FMFMC is unstable equilibrium if;

$$|arg(\lambda_i)| < q\frac{\pi}{2} \tag{12}$$

Using (11) we could show that the FMFMC system is unstable when the fractional-order $q > 0.9$.

3.2. Lyapunov exponents

To calculate the Lyapunov exponents (LEs) of the FMFMC, we use the well-known Wolf's algorithm [51] and a modified solver using the RK4 for the first state and the fractional-order predictor-corrector [50] solver fde12 [50,52,53] for the remaining three states. We used a finite time of 10000s with a step size for integration as 0.01 and the LEs for the FMFMC system are calculated as [0.041;0;-0.0050;-0.14] for fractional-order q=0.98 and parameter values are given in (3).

3.3. Bifurcation

The bifurcation transitions of the FMFMC system is investigated with two approaches: (Case:1) To understand the parameter dependence of the system, we derive and investigate the bifurcation plots for the parameter a_3 variation and other parameter values as shown in (3) with fractional-order $q = 0.98$ (Case:2) For fractional-order and parameter values are taken as in (3).

Case 1: The parameter a_3 is varied with a range $0.1 \leq a_3 \leq 1.3$ to analyze the dynamical behavior of the system. Fig. 3 shows the bifurcation diagram plotted between a_3 against the local maximum value of the state variable y. Numerical simulations are performed through the Runge-Kutta algorithm and fractional-order predictor-corrector solver fde12. The initial condition for the first iteration is taken as [0.041;0;-0.0050;-0.14] and are reinitialized at the end of each iteration to the final values of the state variables. From the bifurcation diagram we could observe that while increasing the parameter till 0.63, the system shows chaotic oscillations. Further increase results with period halving and the system behave with periodic oscillations. In the window from 0.83 to 1.15 again the system enters to chaotic behavior, but we can see some breaks near to 0.85 and 1.12. After the parameter reaches 1.16 slowly the system shows periodic oscillations as period halving occurs. Multistability in FMFMC system can be seen from Fig. 3.a. The evidence of multistability can be seen by comparing the forward (blue color) and backward (red color) bifurcation diagrams. The corresponding coexisting attractors are shown in Figs. 3.b and 3.c.

Case 2: When investigating a fractional-order system, the impact of the order needs to be studied and we present the bifurcation plot of the system. In order to illustrate the bifurcation phenomenon intuitively, we generate the bifurcation of FMFMC system with fractional-order for $0.88 \leq q \leq 1$ range with step size $h = 0.01$ and initial conditions $[0.041; 0; -0.0050; -0.14]$ with reinitializing the initial conditions in every iteration to the end values of the state variables. As can be seen from the bifurcation plot the system shows the period doubling route to chaos for change in fractional-order. System oscillates with chaotic attractor only for $q > 0.94$. Periodic oscillation is observed for the value $q < 0.932$ and for the window $0.9325 \leq q \leq 0.938$ the system shows period doubling oscillation. A small window of periodic oscillation is identified for the value $0.978 \leq q \leq 0.982$ in Fig. 4.

4. Synchronization of the FMFMC system

Pecora and Carroll [54] demonstrated that two identical autonomous chaotic systems can be synchronized with a common signal or signals when the Lyapunov exponent signs for subsystems are all negative. Synchronization means that two identical

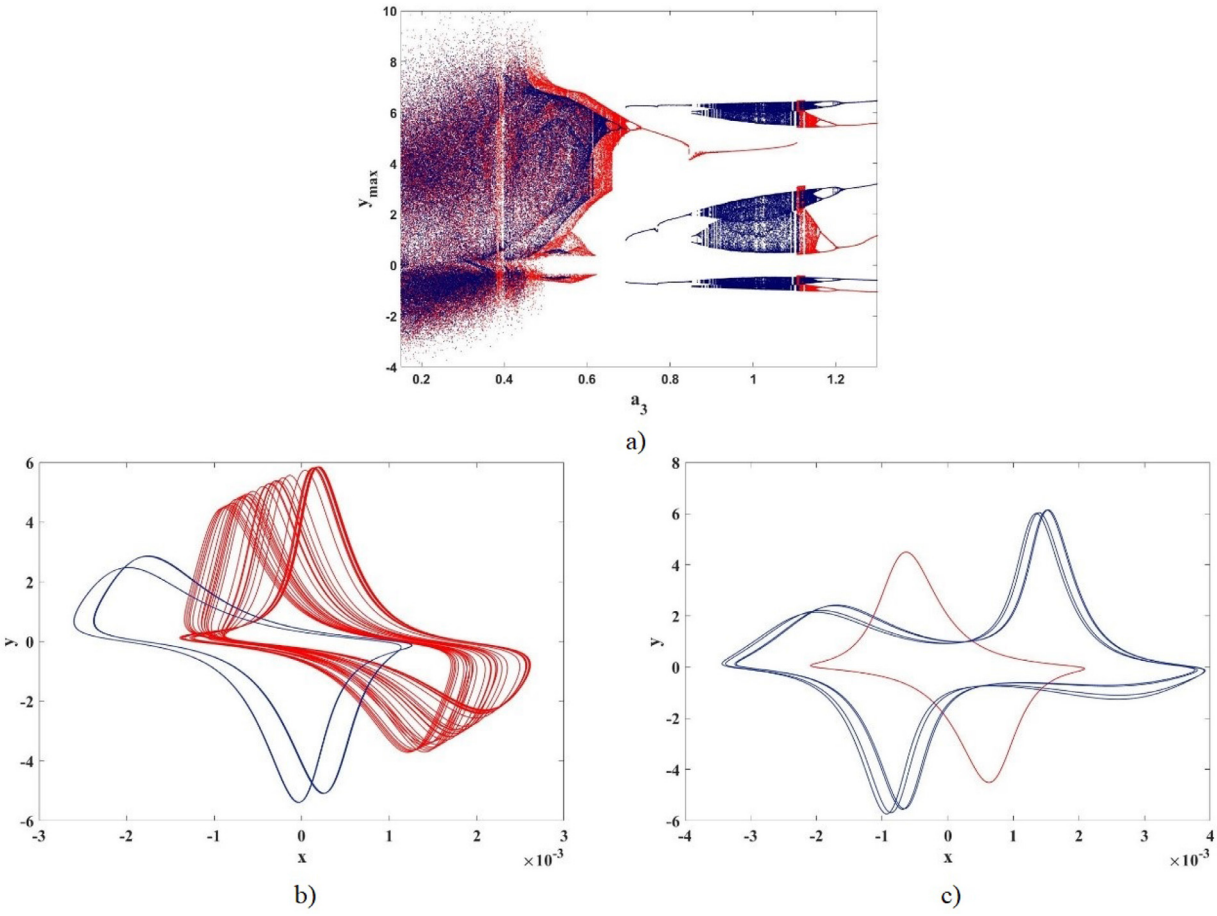

Fig. 3. a) Bifurcation diagram of the FMFMC system with a_3; b) The coexisting attractor for $q = 0.98$ and $a_3 = 0.663$ for the initial conditions $[0; -0.39; 0.01; 42.85]$ shown in red plot and $[-0.001; -0.03; 0.003; 36.12]$ for blue plot; c) The coexisting attractor for $q = 0.98$ and $a_3 = 0.8$ for the initial conditions $[0; 2.9; -0.007; 40.65]$ shown in red plot and $[0; -5.08; 0.01; 35.95]$ shown in blue plot.

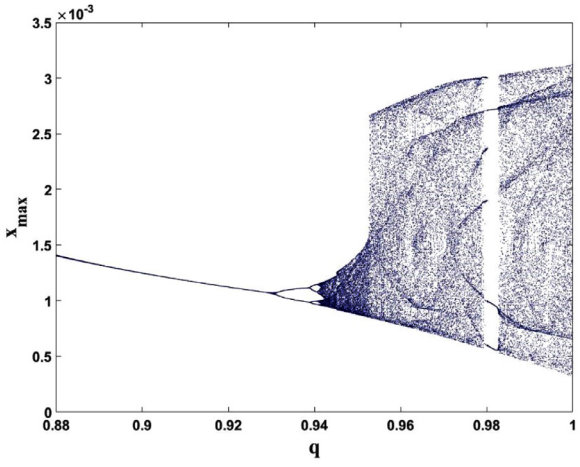

Fig. 4. Bifurcation diagram of the FMFMC system with q.

chaotic systems at different initial conditions come under the same conditions as a common signal and produce the same signals. Pecora and Carroll applied their proposed method to the well-known Lorenz [55] and Rssler [56] chaotic systems. They have also shown that synchronization works in practice by applying it with real circuits [54].

Pecora and Carroll handled the autonomous n-dimensional dynamic system in (13) in their proposed method.

$$\dot{u} = f(u) \tag{13}$$

It is obtained by dividing the system in (13) arbitrarily into two subsystems in the form of [u = (v, w)] (14).

$$\dot{v} = g(v, w), \quad \dot{w} = h(v, w) \tag{14}$$

After this step, they created a new w' system identical to the Pecora-Carroll w system. Here, if (14) is rewritten by replacing the v' variables corresponding to the h function with v, (15) is obtained.

$$\dot{v} = g(v, w), \quad \dot{w} = h(v, w), \quad \dot{w}' = h\left(v, w'\right) \tag{15}$$

Pecora and Carroll studied the difference between the two systems, $\Delta w = w' - w$. These two systems w and w' subsystem components are synchronized only when the difference $\Delta w \to 0$ and $t \to \infty$ for infinite time. At the infinitesimal limit, this is expressed by the variational equations given in (16) for the subsystem [54].

$$\dot{\xi} = D_w h(v(t), w(t))\xi \tag{16}$$

Here $D_w h$ is the Jacobian of the w subsystem vector field with respect to w only. The behavior of (16) or its matrix version [57] depends on the Lyapunov bases of the w subsystem. These are called sub-Lyapunov bases. Accordingly, Pecora and Carroll proposed the following theorem, w and w' subsystems will synchronize only if all of the sub Lyapunov bases are negative [54].

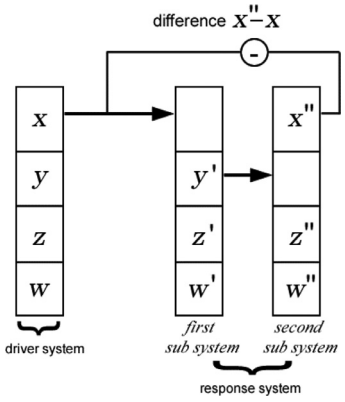

Fig. 5. The block diagram of P-C Synchronization [54].

Pecora-Carroll (P-C) synchronization block diagram in Fig. 5 is given. In Fig. 5, X, Y and Z status variables directly stimulate the subsystem. The response system is divided into two subsystems as X and Y status. The P-C process synchronizes two similar disorderly processes, with separate initial conditions [58]. In the P-C method, when the X status variable in the driver and response system is operated under different starting conditions, the two identical systems synchronize after a certain time. In data communication, the message signal encrypted with the chaotic X status variable in the driver system is transmitted securely to the other party. The X" status variable of the response system on the opposite side is removed from the transmitted encrypted signal and the original message is obtained. This way secure communication is provided. The synchronization of the two systems in the shortest time makes the communication faster and more accurate. Delays prevent communication from being healthy.

In this study, the fractional-order FMFMC system was synchronized using the P-C synchronization method. Although the P-C method is used in integer-order chaotic systems, it also works well in fractional-order systems. Accordingly, no change was made in the working logic of the P-C method, only two identical chaotic integer-order systems were converted to fractional-order system. Here, the P-C method works in the integer-order chaotic system as well as in the fractional-order chaotic system and makes more precise synchronization. The reason for this is fractional-order, the chaotic system gives more sensitive results. Fractional-order chaotic systems synchronize faster in the P-C method compared to integer-order chaotic systems.

In Fig. 6, Matlab Simulink model of the proposed fractional-order system is given. In Matlab Simulink application FMFMC system is modeled with the system Nid toolbox [59]. Nid toolbox is used to perform fractional-order modeling in Matlab Simulink environment. In order to explain the synchronization of the proposed FMFMC system with the P-C method, driver and response equations of the representative chaotic system are given in (17), (18) and (19). The proposed fractional-order chaotic system driver circuit equation of the system is given in (18).

$$\begin{aligned}
\frac{d^q x}{dt^q} &= a_1 M_c z,\\
\frac{d^q y}{dt^q} &= -a_2 M_c z - a_3 y + a_4 M_c^2 z^2 y,\\
\frac{d^q z}{dt^q} &= -x - M_R M_C z,\\
\frac{d^q w}{dt^q} &= z
\end{aligned} \tag{17}$$

The first-order ($\dot{y}$, $\dot{z}$, $\dot{w}$) state variables of the driver system are used in the first sub system of the response system given in (18).

$$\begin{aligned}
\frac{d^q \dot{y}}{dt^q} &= -a_2 M_c \dot{z} - a_3 \dot{y} + a_4 M_c^2 \dot{z}^2 \dot{y},\\
\frac{d^q \dot{z}}{dt^q} &= -x - M_R M_C \dot{z},\\
\frac{d^q \dot{w}}{dt^q} &= \dot{z}
\end{aligned} \tag{18}$$

In the second sub system of the fractional-order chaotic response system given in (19), the $\dot{y}$ state variable in the first subsystem is used in the second-order ($\ddot{x}$, $\ddot{z}$, $\ddot{w}$) state variables [54,58].

$$\begin{aligned}
\frac{d^q \ddot{x}}{dt^q} &= a_1 M_c \ddot{z},\\
\frac{d^q \ddot{z}}{dt^q} &= -\ddot{x} - M_R M_C \ddot{z},\\
\frac{d^q \ddot{w}}{dt^q} &= \ddot{z}
\end{aligned} \tag{19}$$

Finally, in the synchronized fractional-order chaotic response system, $x_r = \ddot{x}$, $y_r = \ddot{y}$, $z_r = \ddot{z}$ and $w_r = \ddot{w}$ are used in the system.

In the P-C synchronization method, identical fractional-order chaotic systems are synchronized using different initial conditions. The initial conditions were selected as $(x_0, y_0, z_0, w_0) = \{0, -4, -0.01, 43\}$ and $(x_r, y_r, z_r, w_r) = \{1, -4, -0.01, 43\}$, respectively.

In this study, a secure communication application was also performed. Identical fractional-order chaotic system synchronized with P-C method is used in secure communication application. In the secure communication application, communication is provided by using synchronized y and y_r state variables.

MATLAB Simulink models of secure communication applications of FMFMC system using P-C method are given in Figs. 8 and 9.

In the chaotic system proposed in Fig. 8, Matlab Simulink model of the secure communication application obtained without using fractional-order is given. In Fig. 9, Matlab Simulink model of the secure communication application obtained using fractional-order is given. The only difference between the two Matlab Simulink models in Figs. 8 and 9 is that the Nid function [59] is used in one and not in the other. The fractional-order function is provided through the Nid function. While secure communication application is made in Figs. 8 and 9, driver and receiver systems are designed by using P-C synchronization in Fig. 5. In both Figs. 8 and 9, the driver system is shown with a blue frame, the response system with a green frame and the secure communication application with a red frame. The receiving system is divided into two subsystems. In the first subsystem, x state variable is provided from the driver system, while in the second subsystem, y state variable is provided from the first subsystem. The synchronization applications in both Fig. 8 and Fig. 9 provide secure communication. However, the delay time is shorter in the synchronization application using fractional-order.

A new fractional chaotic system has been established as the chaotic method of encrypted data transmission for secure communication and the relevant equations are given in (20). The equations of the transmitter circuit are given in (20).

$$\begin{aligned}
\frac{d^q \dot{x}_r}{dt^q} &= a_1 M_c z,\\
\frac{d^q \dot{y}_r}{dt^q} &= -a_2 M_c z - a_3 y + a_4 M_c^2 z^2 y,\\
\frac{d^q \dot{z}_r}{dt^q} &= -s(t) - M_R M_C z,\\
\frac{d^q \dot{w}_r}{dt^q} &= z
\end{aligned} \tag{20}$$

The principle scheme of the chaotic information hiding method is given in Fig. 7. The sine signal $i(t)$ with a value of 10V-amplitude

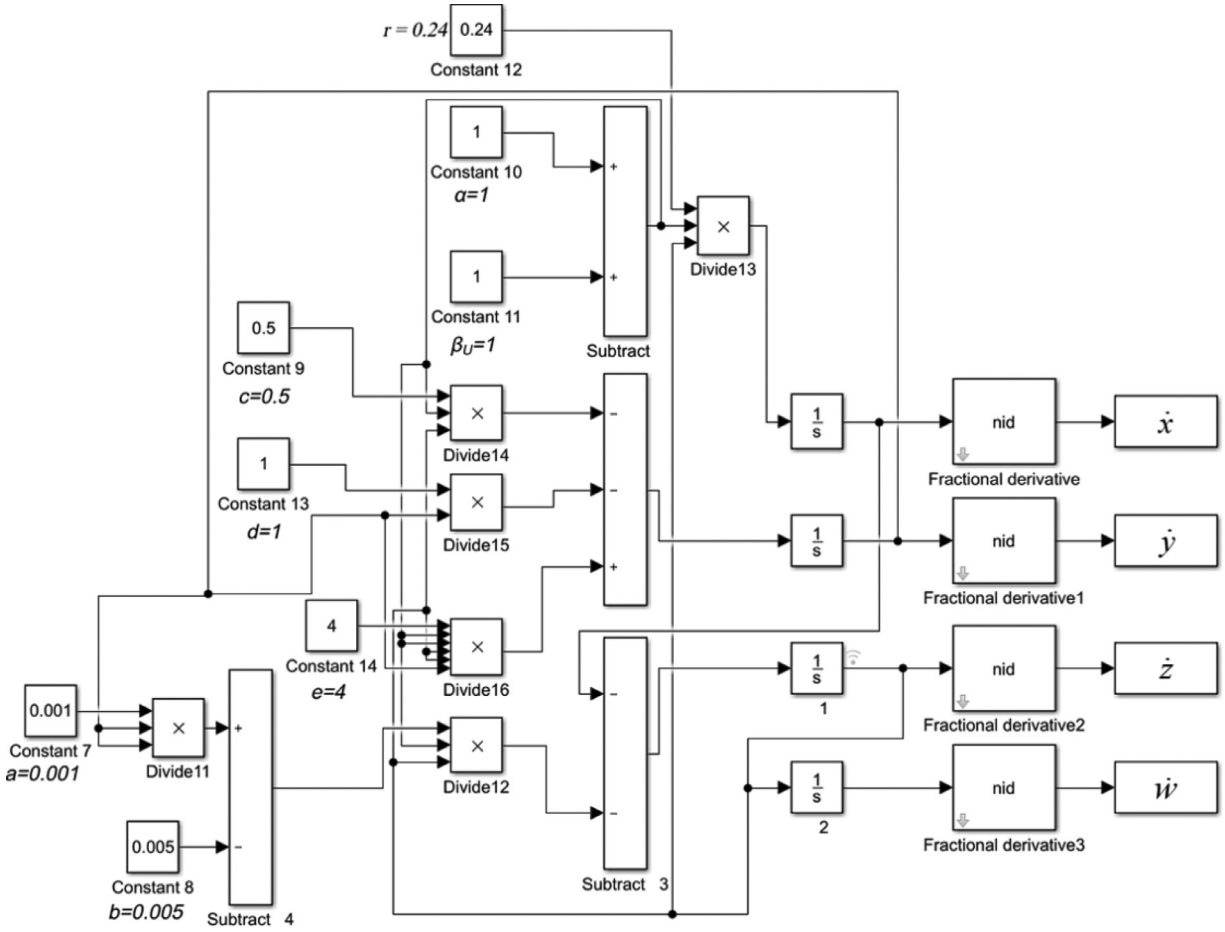

Fig. 6. Matlab Simulink model of FMFMC system.

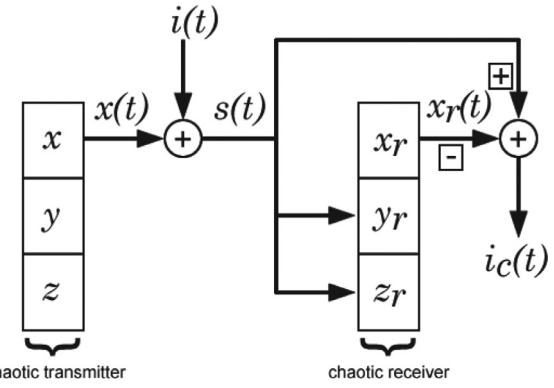

Fig. 7. Principle scheme for chaotic secure communication [60].

is sent through the FMFMC system. The information signal $i(t)$ is summed with the chaotic signal $(x(t))$ and the signal $s(t)$ obtained is transmitted to the communication line. The chaotic signal obtained from the y_r (response system) state variable is extracted from the encrypted signal $s(t)$. The received signal $i_c(t)$ is obtained. The difference between the sent $i(t)$ signal and the received $i_c(t)$ signal indicates the secure communication (esc) error. The difference of y_r and y status variables gives synchronization error (esy).

Using the Matlab Simulink models in Figs. 8 and 9, the FMFMC system phase portraits without $(q = 1)$ and with $(q = 0.98)$ fractional-order are given in Fig. 10. The $X - Y$ phase portrait taken without a fractional-order and the proposed fractional-order system $X - Y$ phase portrait with a value of $q = 0.98$ display different chaotic behaviors. When $q = 0.98$, the density of the x axis increases in negative values. On the contrary, in the phase portrait received without using $q = 1$ fractional-order, the density of the positive values of the x axis increases. In the FMFMC system, $a_1 = 0.24, a_2 = 0.5, a_3 = 1, a_4 = 4, \alpha = \beta = 1, \chi = 0.001$ and $\delta = 0$ was taken. There are four state equations: x, y, z and w.

In Fig. 11, the FMFMC system (q = 1 and q = 0.98) synchronization error graphs synchronized with the P-C method are given. In Fig. 11.a, graphs of error signals resulting from secure communication and proposed system synchronization without fractional-order are given. In Fig. 11.b, graphs of the error signals resulting from the secure communication and proposed system synchronization with fractional-order are given. In all graphics, the error caused by Esy and the error caused by Esc created a mirror image due to the compatibility between each other. The proposed system without fractional-order (q = 1) is synchronized in 13.5 time units (Fig. 11.a), and with fractional-order (q = 0.98) - in 13.1 time units (Fig. 11.b). In the FMFMC system, the fractional-order value only affected 0.4 time units.

Time-Error analysis is given in Table 1 to theoretically analyze the secure communication error (Esc) and variable y synchronization error (Esy) values of integer-order and fractional-order (q = 0.98) of the proposed chaotic FMFMC system. In the Table 1, the process until the FMFMC system is synchronized in both cases between $1 - 13.5$ms time value is examined. The integer-order

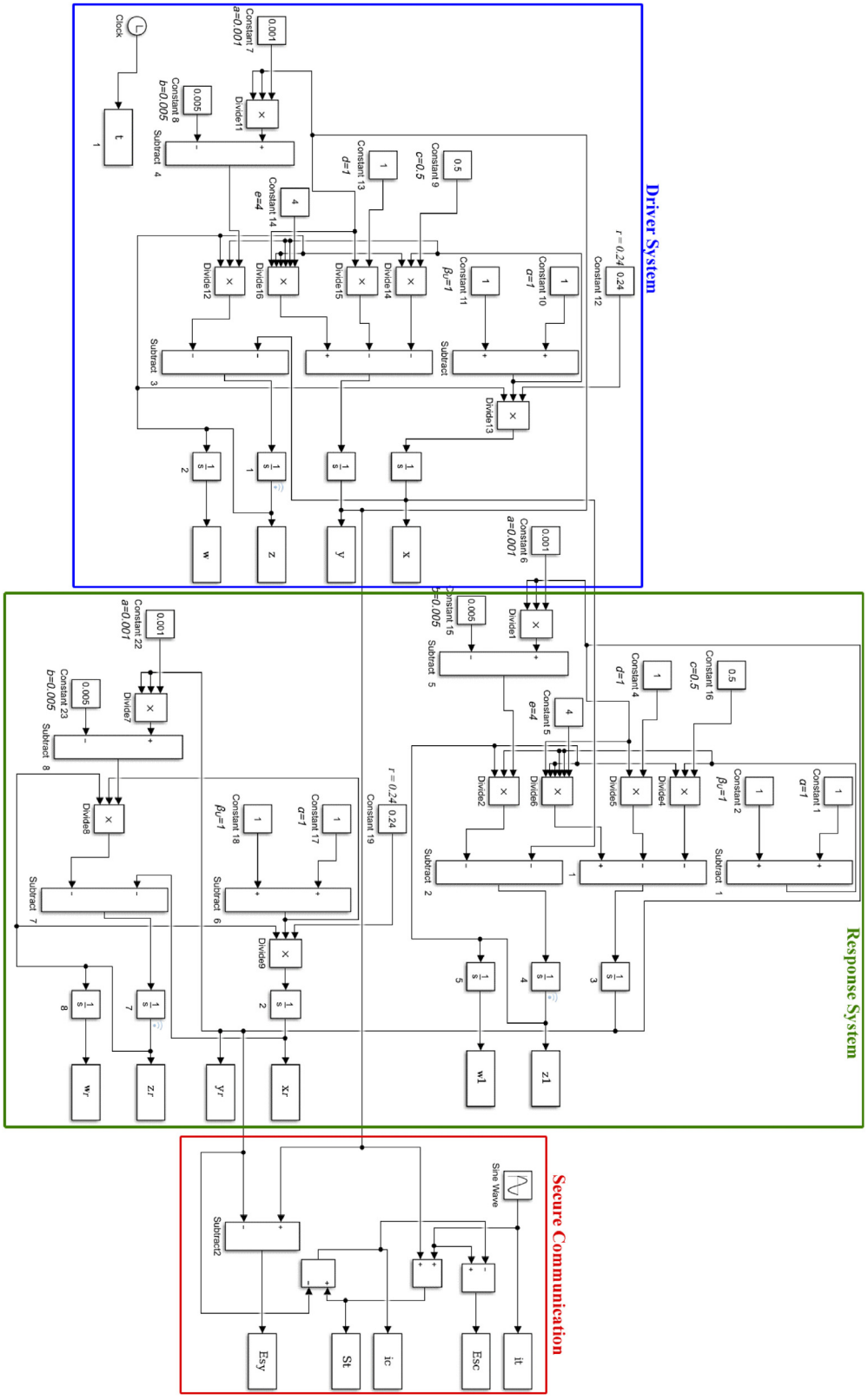

Fig. 8. Matlab Simulink model of secure communication proposed system without fractional-order.

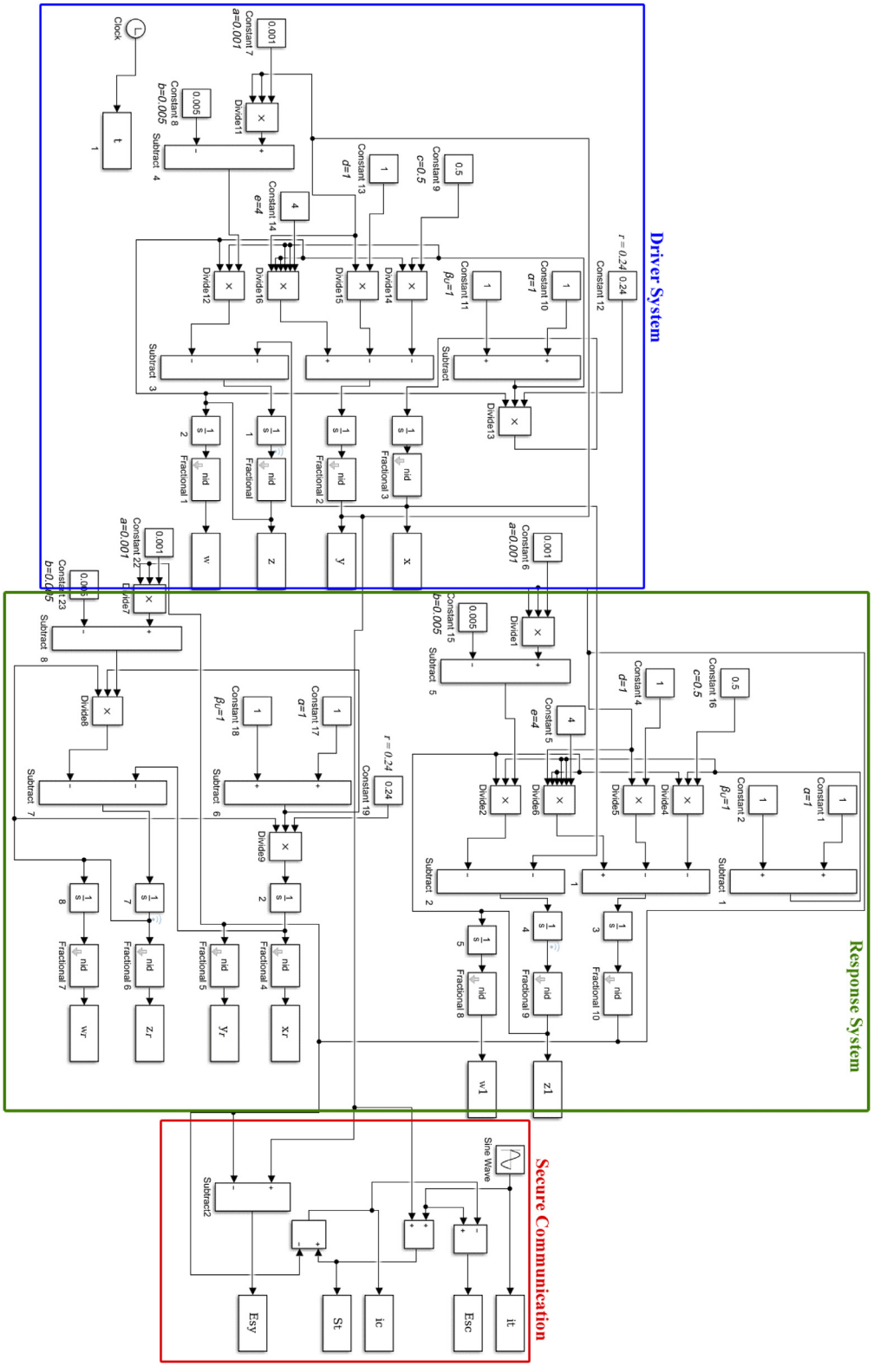

Fig. 9. Matlab Simulink model of secure communication FMFMC system.

system synchronized in 13.5 ms (which is 0.04 ms longer than the fractional-order system). Both the fractional-order and integer-order systems are synchronized sinusoidally, with error values approaching zero. Fractional order systems work more precisely because of their fractional structure and synchronize the chaotic system faster.One of the reasons why the results are so close to each other is that the complex structure of the state variables in the equation of the FMFMC system causes the chaotic system to behave almost like fractional-order, even when integer-order is used. The fact that Esc and Esy error values are parallel to each other in all values is an important proof that the systems are synchronized.

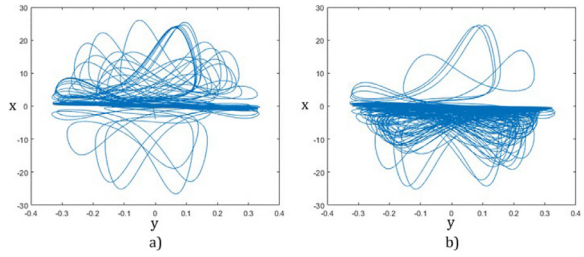

Fig. 10. 2D state portraits (xy planes) of FMFMC system with different q values ($q = 1$ and $q = 0.98$): a) $q = 1$ without fractional-order, b) $q = 0.98$ with fractional-order.

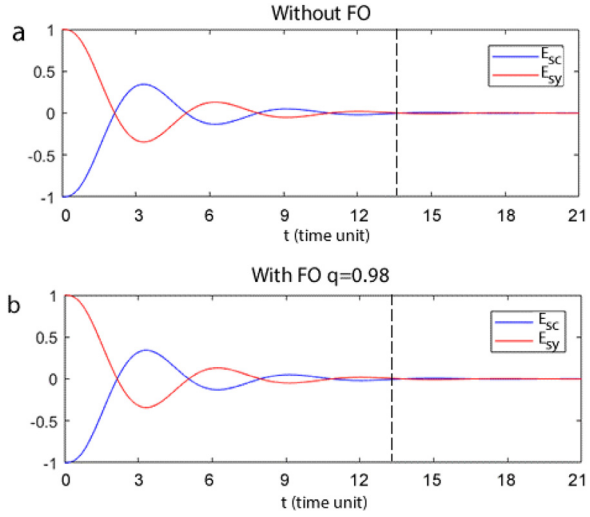

Fig. 11. Synchronization error of FMFMC system (q=1 and q=0.98).(Esc - secure communication error, Esy - variable y synchronization error); a) without fractional-order (q=1); b) with fractional-order (q=0.98).

Table 1
Time-Error analysis of integer-order and fractional-order FMFMC system.

	Integer-Order		Fractional-Order	
Time (ms)	Esc	Esy	Esc	Esy
1	-0.86	0.86	-0.81	0.81
2	-0.22	0.22	-0.18	0.18
3	0.32	-0.32	0.25	-0.25
6	-0.11	0.11	-0.09	0.09
9	0.07	-0.07	0.05	-0.05
12	-0.04	0.04	-0.02	0.02
13.1	0.02	-0.02	0	0
13.5	0	0	0	0

5. Conclusion

While the existing studies in the literature do not include fractional-order systems, in this study the system was studied as fractional order. In the study, memristor and memcapacitor elements were used together and synchronization application was made.In this paper, we presented a novel fractional-order chaotic system based on memristor-memcapacitor with a linear inductor. The dynamical analysis results showed the complexity of the system and sensitivity to various parameters. Stability analysis, bifurcation and Lyapunov exponents are used to discuss behavioral changes for different scenario of the circuit. We proposed a synchronization methodology to synchronize the master and slave fractional-order systems and implement the system in secure communication. The presence of rich dynamical behaviors showed the system is suitable for various applications such as random number generator, cryptography and data hiding. The simplicity in system structure will allow us to overcome the challenges in real time application.

Availability of data

The data that support the findings of this study are available from the corresponding author upon reasonable request.

Declaration of Competing Interest

The authors declare that they have no conflict of interest.

Acknowledgements

This work was supported by Sakarya University of Applied Science Scientific Research Projects Coordination Unit (SUBU BAPK, Project Number: 2020-01-01-011). The author, Muhammed Ali PALA, is grateful to The Scientific and Technological Research Council of Turkey for granting a scholarship (TUBITAK, 2211-C) for him Ph.D. studies.

Appendix-1

The current through a voltage controlled memristor can be defined as [1]

$$\begin{aligned} i_{M_R^q} &= M_R^q V_{M_R^q} \\ D^q y &= -a_2 V_{M_R^q} - a_3 y + a_4 V_{M_R^q}^2 y. \\ M_R^q &= \chi y^2 - \delta \end{aligned} \tag{A-1}$$

where $i_{M_R^q}, V_{M_R^q}, M_R^q$ represents the current, voltage and the memresistance of the voltage controlled memristor.

Similarly, by the definition of memcapacitor [61], the expression of memcapacitance in a charge controlled memcapacitor is

$$\begin{aligned} V(t)_{M_C^q} &= M_C^q Q(t)_{M_C^q} \\ M_C^q &= \alpha + \beta w \\ Q(\tau)_{M_C^q} &= {}_{t_0}^{t} D^q w(\tau) \end{aligned} \tag{A-2}$$

where $V_{M_C^q}$ and $Q_{M_C^q}$ represents the voltage and charge of the memcapacitor at time t. The rate of change of state w represents the charge in the memcapacitor at time τ.

From Fig. 1, we could derive the state equations using Kirchhoff's Voltage Law and Kirchhoff's Current Law considering the current across the inductor i_L, memristor internal state (y), the flux (ϕ) and the internal state of memcapacitor (w) as the states as below

$$\begin{aligned} \dot{i}_L &= \frac{1}{L} M_C^q \phi \\ D^q y &= -a_2 M_C^q \phi - a_3 y + a_4 M_C^{q^2} \phi^2 y \\ D^q \phi &= -i_L - M_R^q M_C^q \phi \\ D^q w &= \phi \\ M_C^q &= \alpha + \beta w \\ M_R^q &= \chi y^2 - \delta \end{aligned} \tag{A-3}$$

References

[1] Chua LO. Memristor-the missing circuit element. IEEE Trans Circuit Theory 1971;18:507–19.
[2] Stanley Williams R. How we found the missing memristor. In: Chaos, CNN, Memristors and Beyond: A Festschrift for Leon Chua With DVD-ROM, composed by Eleonora Bilotta. World Scientific; 2013. p. 483–9.
[3] Vourkas I, Sirakoulis GC. Emerging memristor-based logic circuit design approaches: a review. IEEE Circuit Syst Mag 2016;16(3):15–30.

[4] Abbas H, Abbas Y, Truong SN, Min K-S, Park MR, Cho J, et al. A memristor crossbar array of titanium oxide for non-volatile memory and neuromorphic applications. Semiconductor Sci. Technol. 2017;32(6):065014.
[5] Dong Z, Lai CS, He Y, Qi D, Duan S. Hybrid dual-complementary metal–oxide–semiconductor/memristor synapse-based neural network with its applications in image super-resolution. IET Circuit. Dev Syst 2019;13(8):1241–8.
[6] Mikhaylov A, Pimashkin A, Pigareva Y, Gerasimova S, Gryaznov E, Shchanikov S, et al. Neurohybrid memristive cmos-integrated systems for biosensors and neuroprosthetics. Front Neurosci 2020;14:358.
[7] Guarcello C, Valenti D, Carollo A, Spagnolo B. Effects of lévy noise on the dynamics of sine-gordon solitons in long josephson junctions. J Stat Mech: Theory Exp. 2016;2016(5):054012.
[8] Sharifi MJ, Banadaki YM. General spice models for memristor and application to circuit simulation of memristor-based synapses and memory cells. J Circuit Syst Comput 2010;19(02):407–24.
[9] Iu HH-C, Yu D, Fitch AL, Sreeram V, Chen H. Controlling chaos in a memristor based circuit using a twin-t notch filter. IEEE Trans Circuit Syst I 2011;58(6):1337–44.
[10] Wu R, Wang C. A new simple chaotic circuit based on memristor. Int J Bifurcat Chaos 2016;26(09):1650145.
[11] Pizzolato N, Fiasconaro A, Adorno DP, Spagnolo B. Resonant activation in polymer translocation: new insights into the escape dynamics of molecules driven by an oscillating field. Phys Biol 2010;7(3):034001.
[12] Ma X, Mou J, Liu J, Ma C, Yang F, Zhao X. A novel simple chaotic circuit based on memristor–memcapacitor. Nonlinear Dyn 2020;100(3):2859–76.
[13] Khater MM, Almohsen B, Baleanu D, Inc M. Numerical simulations for the predator–prey model as a prototype of an excitable system. Numer Method Partial Diff Eqs 2020.
[14] Denaro G, Valenti D, La Cognata A, Spagnolo B, Bonanno A, Basilone G, et al. Spatio-temporal behaviour of the deep chlorophyll maximum in mediterranean sea: development of a stochastic model for picophytoplankton dynamics. Ecol Complex 2013;13:21–34.
[15] Denaro G, Valenti D, Spagnolo B, Basilone G, Mazzola S, Zgozi SW, et al. Dynamics of two picophytoplankton groups in mediterranean sea: analysis of the deep chlorophyll maximum by a stochastic advection-reaction-diffusion model. PLoS One 2013;8(6):e66765.
[16] Dubkov AA, Spagnolo B. Acceleration of diffusion in randomly switching potential with supersymmetry. Phys Rev E 2005;72(4):041104.
[17] Fiasconaro A, Valenti D, Spagnolo B. Role of the initial conditions on the enhancement of the escape time in static and fluctuating potentials. Phys A 2003;325(1-2):136–43.
[18] Spagnolo B, Dubkov A, Pankratov A, Pankratova E, Fiasconaro A, Ochab–Marcinek A. Lifetime of metastable states and suppres- sion of noise in interdisciplinary physical models. Acta Phys Pol B, Vol 38, 1925-1950 2007.
[19] Zhou L, Wang C, Zhou L. Generating four-wing hyperchaotic attractor and two-wing, three-wing, and four-wing chaotic attractors in 4d memristive system. Int J Bifurcat Chaos 2017;27(02):1750027.
[20] Carollo A, Spagnolo B, Valenti D. Uhlmann curvature in dissipative phase transitions. Sci Rep 2018;9852. doi:10.1038/s41598-018-27362-9. 8.
[21] Ma J, Chen Z, Wang Z, Zhang Q. A four-wing hyper-chaotic attractor generated from a 4-d memristive system with a line equilibrium. Nonlinear Dyn 2015;81(3):1275–88.
[22] Bao B, Bao H, Wang N, Chen M, Xu Q. Hidden extreme multistability in memristive hyperchaotic system. Chaos Soliton Fractal 2017;94:102–11.
[23] Lü J, Chen G. A new chaotic attractor coined. Int J Bifurcat chaos 2002;12(03):659–61.
[24] Li Q, Zeng H, Li J. Hyperchaos in a 4d memristive circuit with infinitely many stable equilibria. Nonlinear Dyn 2015;79(4):2295–308.
[25] Njitacke Z, kengne J, Fotsin H, Negou AN, Tchiotsop D. Coexistence of multiple attractors and crisis route to chaos in a novel memristive diode bidge-based jerk circuit. Chaos Soliton Fractal 2016;91:180–97.
[26] Njitacke Z, Kengne J, Tapche RW, Pelap F. Uncertain destination dynamics of a novel memristive 4d autonomous system. Chaos Soliton Fractal 2018;107:177–85.
[27] Kuate PDK, Lai Q, Fotsin H. Complex behaviors in a new 4d memristive hyperchaotic system without equilibrium and its microcontroller-based implementation. Eur Phys J Spec Topics 2019;228(10):2171–84.
[28] Sahin ME, Taskiran ZGC, Guler H, Hamamci SE. Application and modeling of a novel 4d memristive chaotic system for communication systems. Circuit Syst Signal Process 2020:1–30.
[29] Khalil NA, Fouda ME, Said LA, Radwan AG, Soliman AM. A general emulator for fractional-order memristive elements with multiple pinched points and application. AEU-Int J Electron Commun 2020;124:153338.
[30] Ma C, Mou J, Li P, Yang F, Liu T. Multistability analysis and digital circuit implementation of a new conformable fractional-order chaotic system. Mobile Networks and Applications 2020:1–10.
[31] Xu B, Wang G, Shen Y. A simple meminductor-based chaotic system with complicated dynamics. Nonlinear Dyn 2017;88(3):2071–89.
[32] Mou J, Sun K, Ruan J, He S. A nonlinear circuit with two memcapacitors. Nonlinear Dyn 2016;86(3):1735–44.
[33] Filatov D, Vrzheshch D, Tabakov O, Novikov A, Belov A, Antonov I, et al. Noise-induced resistive switching in a memristor based on zro2 (y)/ta2o5 stack. J Stat Mech 2019;2019(12):124026.
[34] Giuffrida A, Valenti D, Ziino G, Spagnolo B, Panebianco A. A stochastic interspecific competition model to predict the behaviour of listeria monocytogenes in the fermentation process of a traditional sicilian salami. Eur Food Res Technol 2009;228(5):767–75.
[35] Mikhaylov A, Gryaznov E, Belov A, Korolev D, Sharapov A, Guseinov D, et al. Field-and irradiation-induced phenomena in memristive nanomaterials. Phys Status Solidi (c) 2016;13(10-12):870–81.
[36] Spagnolo B, La Barbera A. Role of the noise on the transient dynamics of an ecosystem of interacting species. Phys A 2002;315(1-2):114–24.
[37] Spagnolo B, Valenti D. Volatility effects on the escape time in financial market models. Int J Bifurcat Chaos 2008;18(09):2775–86.
[38] Rajagopal K, Jafari S, Karthikeyan A, Srinivasan A, Ayele B. Hyperchaotic memcapacitor oscillator with infinite equilibria and coexisting attractors. Circuit Syst Signal Process 2018;37(9):3702–24.
[39] Li P, Xu J, Mou J, Yang F. Fractional-order 4d hyperchaotic memristive system and application in color image encryption. EURASIP J Image Video Process 2019;2019(1):22.
[40] Tsafack N, Kengne J, Abd-El-Atty B, Iliyasu AM, Hirota K, Abd EL-Latif AA. Design and implementation of a simple dynamical 4-d chaotic circuit with applications in image encryption. Inf Sci 2020;515:191–217.
[41] Toopchi Y, Wang J. Chaos control and synchronization of a hyperchaotic zhou system by integral sliding mode control. Entropy 2014;16(12):6539–52.
[42] Lu J, Wu X, Lü J. Synchronization of a unified chaotic system and the application in secure communication. Phys Lett A 2002;305(6):365–70.
[43] Rajchakit G, Chanthorn P, Niezabitowski M, Raja R, Baleanu D, Pratap A. Impulsive effects on stability and passivity analysis of memristor-based fractional-order competitive neural networks. Neurocomputing 2020;417:290–301.
[44] Ma X, Mou J, Liu J, Ma C, Yang F, Zhao X. A novel simple chaotic circuit based on memristor–memcapacitor. Nonlinear Dyn 2020;100(3):2859–76.
[45] Zhou P, Ma J, Tang J. Clarify the physical process for fractional dynamical systems. Nonlinear Dyn 2020;100(3):2353–64.
[46] Rajagopal K, Li C, Nazarimehr F, Karthikeyan A, Duraisamy P, Jafari S. Chaotic dynamics of modified wien bridge oscillator with fractional order memristor. Radioengineering 2019;28(1):165–74.
[47] Yu Y, Wang Z. Initial state dependent nonsmooth bifurcations in a fractional-order memristive circuit. Int J Bifurcat Chaos 2018;28(07):1850091.
[48] Diethelm K. An algorithm for the numerical solution of differential equations of fractional order. Electron Trans Numer Anal 1997;5(1):1–6.
[49] Diethelm K, Ford NJ. Analysis of fractional differential equations. J Math Anal Appl 2002;265(2):229–48.
[50] Sun H, Abdelwahab A, Onaral B. Linear approximation of transfer function with a pole of fractional power. IEEE Trans Autom Control 1984;29(5):441–4.
[51] Diethelm K, Freed AD. The fracpece subroutine for the numerical solution of differential equations of fractional order. Forschung und wissenschaftliches Rechnen 1998;1999:57–71.
[52] Roberto garrappa (2020). predictor-corrector pece method for fractional differential equations (https://www.mathworks.com/matlabcentral/fileexchange/32918-predictor-corrector-pece-method-for-fractional-differential-equations), matlab central file exchange. retrieved october 22, 2020.
[53] Wolf A, Swift JB, Swinney HL, Vastano JA. Determining lyapunov exponents from a time series. Physica D: Nonlinear Phenomena 1985;16(3):285–317.
[54] Pecora LM, Carroll TL. Synchronization in chaotic systems. Phys Rev Lett 1990;64(8):821.
[55] Lorenz EN. Deterministic nonperiodic flow. J Atmospher. Sci 1963;20(2):130–41.
[56] Rossler O. Phys Lett A 1976;57:397–8.
[57] Guckenheimer J, Holmes P. Nonlinear oscillations, dynamical systems, and bifurcations of vector fields 2013;42.
[58] Pecora LM, Carroll TL. Driving systems with chaotic signals. Phys Rev A 1991;44(4):2374.
[59] Sheng H, Chen Y, Qiu T. Fractional processes and fractional-order signal processing: techniques and applications. Springer Science & Business Media; 2011.
[60] Pehlivan I, Uyaroglu Y. Simplified chaotic diffusionless lorentz attractor and its application to secure communication systems. IET Commun 2007;1(5):1015–22. doi:10.1049/iet-com:20070131.
[61] Wang G-Y, Cai B-Z, Jin P-P, Hu T-L. Memcapacitor model and its application in a chaotic oscillator. Chinese Phys B 2015;25(1):010503.